

# Imaging the Sunyaev-Zel'dovich Effect

J. E. Carlstrom<sup>1</sup>, M. K. Joy<sup>2</sup>, L. Grego<sup>3</sup>, G. P. Holder<sup>1</sup>,  
W. L. Holzapfel<sup>4</sup>, J. J. Mohr<sup>1</sup>, S. Patel<sup>5</sup>, and E. D. Reese<sup>1</sup>

*to appear in the proceedings of the Nobel Symposium "Particle Physics and the Universe"*  
*Physica Scripta and World Scientific, eds. L. Bergstrom, P. Carlson and C. Fransson*

## Abstract

We report on results of interferometric imaging of the Sunyaev-Zel'dovich Effect (SZE) with the OVRO and BIMA mm-arrays. Using low-noise cm-wave receivers on the arrays, we have obtained high quality images for 27 distant galaxy clusters. We review the use of the SZE as a cosmological tool. Gas mass fractions derived from the SZE data are given for 18 of the clusters, as well as the implied constraint on the matter density of the universe,  $\Omega_M$ . We find  $\Omega_M h_{100} \leq 0.22^{+0.05}_{-0.03}$ . A best guess for the matter density obtained by assuming a reasonable value for the Hubble constant and also by attempting to account for the baryons contained in the galaxies as well as those lost during the cluster formation process gives  $\Omega_M \sim 0.25$ . We also give preliminary results for the Hubble constant. Lastly, the power for investigating the high redshift universe with a non-targeted high sensitivity SZE survey is discussed and an interferometric survey is proposed.

## 1 The Sunyaev-Zel'dovich Effect

The scattering of Cosmic Microwave Background (CMB) photons by a hot thermal distribution of electrons leads to a unique distortion of the CMB spectrum known as the Sunyaev-Zel'dovich Effect (SZE) after the two Russian scientists who proposed it in the early 1970's (Sunyaev and Zel'dovich 1970; Sunyaev and Zel'dovich 1972). In most cases, and in all cases considered here, the hot gas is provided by the intracluster medium of galaxy clusters. For the most massive clusters the mass of the intracluster medium greatly exceeds the mass contained in the individual galaxies, although, as discussed in detail below, roughly 85% of the mass of a cluster is contained in some other form of non-luminous matter. Even for the largest clusters with  $\sim 10^{15} M_\odot$  total mass the chance of a scattering a CMB photon traversing the cluster is only about 1%. This means that the resulting spectral distortion will have a small amplitude.

The photons that scatter off the much higher energy electrons ( $T_e \sim 10^8$  K, 10 keV), will on average be shifted to higher energy. The emergent spectrum is therefore distinctly non-Planckian; compared to an initial Planck spectrum there are fewer photons at low energies and more at high energies. The spectral distortion is shown in Fig. 1 where the left panel shows the change in intensity and the right panel shows the change in Rayleigh Jeans (RJ) brightness temperature. The RJ brightness is shown because the sensitivity of radio telescope is calibrated in these units. It is defined simply by  $I_\nu = (2k\nu^2/c^2)T_{RJ}\Omega$  where  $I_\nu$  is the intensity at frequency  $\nu$ ,  $k$  is Boltzmann's constant,  $\Omega$  is the solid angle and  $c$  is the speed of light. The Planck spectrum of the CMB radiation is also shown by the dotted line in Fig. 1 for reference.

Also shown in Fig. 1 by the dashed curve is the kinetic SZE. This effect is caused by a non-zero bulk velocity of the cluster with respect to the CMB and along the line of sight; a peculiar velocity with respect to the Hubble flow. It results in a purely thermal distortion of the CMB spectrum (i.e., the emergent spectrum is still described completely by a Planck spectrum, but at a slightly different temperature, lower (higher) for positive (negative) peculiar velocities.

The derivation of the exact spectral dependence of SZE can be found in the original papers of Sunyaev and Zel'dovich as well as in a number of more recent papers, which include relativistic corrections to the earlier work, and reviews (e.g., Sunyaev and Zel'dovich 1970; Sunyaev and Zel'dovich 1972; Sunyaev and Zel'dovich 1980; Rephaeli 1995; Birkinshaw 1999).

At long wavelengths, the SZE toward massive and luminous galaxy clusters should be observed as a hole in the sky relative to the undistorted CMB brightness. This in itself is a remarkable feature. There is no

<sup>1</sup>University of Chicago, Department of Astronomy and Astrophysics, 5640 S. Ellis Avenue, Chicago, IL, 60637

<sup>2</sup>NASA/MSFC, Huntsville, AL, 35812

<sup>3</sup>Harvard-Smithsonian Center for Astrophysics, Cambridge, MA, 02138

<sup>4</sup>University of California, Department of Physics, Berkeley, CA, 9472

<sup>5</sup>University of Alabama, Department of Physics, Huntsville, AL, 35899

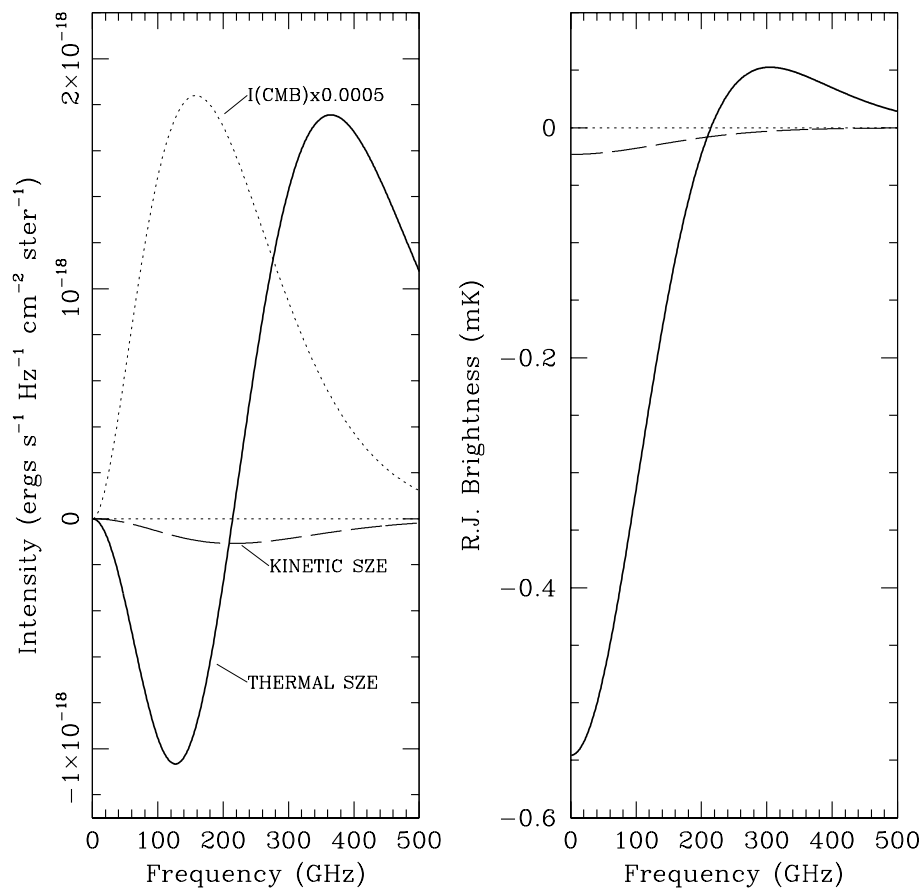


Figure 1: Spectral distortion of the Cosmic Microwave Background (CMB) radiation due to the Sunyaev-Zel'dovich Effect (SZE). The left panel shows the intensity and the right panel shows the Rayleigh Jeans brightness temperature. The thick solid line is the thermal SZE and the dashed line is the kinetic SZE. For reference the 2.7 K thermal spectrum for the CMB intensity scaled by 0.0005 is shown by the dotted line in the left panel; a line at zero is shown in both panels. The cluster properties used to calculate the spectra are an electron temperature of 10 keV, a Compton  $y$  parameter of  $10^{-4}$  and a peculiar velocity of  $500 \text{ km s}^{-1}$ .

other plausible explanation known for the existence of such a hole other than primary CMB anisotropy which should have much smaller amplitudes at the angular scales subtended by galaxy clusters (e.g., Holder and Carlstrom 1999). A clear detection of a SZE decrement was proposed as proof that the CMB was indeed cosmic (Sunyaev and Zel'dovich 1970); if proof is still needed we now know that it at least comes to us from beyond  $z = 0.83$ .

In the Rayleigh-Jeans (RJ) limit the SZE spectral distortion is given by

$$\frac{\Delta T}{T_{CMB}} = -2 \int \frac{kT_e}{m_e c^2} \sigma_T n_e dl \quad (1)$$

where  $T_{CMB}$  is the radiation temperature of the CMB,  $k$  is Boltzmann's constant,  $n_e$  and  $T_e$  are the electron density and temperature, respectively,  $\sigma_T$  is the Thompson cross section,  $m_e$  is the mass of the electron,  $c$  is the speed of light and the integral is along the line of sight. Using the definition for the Comptonization parameter  $y$ , we find that  $\frac{\Delta T}{T_{CMB}} = -2y$  in the RJ limit.

Perhaps the most amazing fact of the SZE is best illustrated by Eq. 1; the observed brightness of the effect  $\Delta T$  is independent of the distance (redshift) to the cluster! Both  $\Delta T$  and  $T_{CMB}$  suffer the same cosmological

dimming, so their ratio is simply a function of the cluster properties. And, of course, we observe the same  $T_{CMB}$  toward any cluster at any redshift. The integrated SZE flux from a cluster depends on  $\Delta T D_A^{-2}$  and is thus dependent on distance. For observations in which the angular resolution is sufficient to resolve the effect, however, the observable is independent of redshift. This requirement is obtained easily, as clusters are large objects ( $\sim$ Mpc) and therefore subtend an arcminute or more at any redshift, assuming a reasonable cosmology. This wonderful property of the SZE makes it a potentially powerful probe of the high redshift universe.

As discussed in section 2, sensitive observations of the SZE provide a powerful and unique cosmological tool. Our group has used interferometric techniques to make high quality images of the SZE toward more than 25 clusters with redshifts spanning 0.13 to 0.83. In section 3, we give a brief review of our observing technique and present some of the resulting images. We discuss our progress on the Hubble constant and mass density of the universe in section 4, and finally in section 5 we briefly review our future plans.

## 2 Cosmology with the Sunyaev-Zel'dovich Effect

Beyond the novelty of measuring a hole in the sky, or adding to the already overwhelming evidence that the CMB is indeed cosmic, measurements of the SZE offer a powerful and unique way to test cosmological models and determine the values of the cosmological parameters which describe our universe.

Here we concentrate on the SZE from galaxy clusters, the largest known collapsed objects in the universe. Galaxy clusters themselves provide important sign-posts of structure in the universe. Their properties and evolution provide valuable constraints on cosmological models. In addition to its SZE, the hot intracluster gas is traced by its strong bremsstrahlung radiation at X-ray wavelengths. The deep gravitational potential can be probed by X-ray spectroscopy (to measure of the intracluster gas temperature), by the velocity dispersion of member galaxies, and by the gravitational lensing of background galaxies.

We now discuss briefly the cosmological probes that are offered directly by SZE measurements of clusters, both by itself and when used in conjunction with the measurements discussed above.

### 2.1 Hubble constant; expansion history of the universe

Perhaps the SZE is best known for providing a means to measure the distance to a galaxy cluster independent of any other distance scale; it does not require normalization to distances derived for more nearby objects as is the case with the ‘‘distance ladder’’ that is commonly used. The distance is derived by combining a measurement of the SZE with a measurement of the X-ray intensity of the cluster. To understand how this is possible it is only necessary to consider the different dependencies of the SZE and X-ray observables on the electron density of the intracluster gas.

The SZE is simply dependent on the integrated density as indicated in Eq. 1. The X-ray intensity is proportional to the density squared as given by

$$I_X(E, \delta_E) = \frac{1}{4\pi(1+z)^4} \frac{\mu_e}{\mu_H} \int n_e^2 \Lambda(E', \delta'_E, T_e) dl \quad (2)$$

where  $I_X(E, \delta_E)$  is the X-ray intensity observed within a fixed detector bandwidth  $\delta_E$  at energy  $E$ ,  $\mu_j \equiv \rho/(n_j m_p)$ ,  $\rho$  is the gas mass density,  $m_p$  is the mass of the proton,  $\Lambda(E', \delta'_E, T_e)$  is the emissivity within a bandwidth  $\delta'_E$  at energy  $E'$  of a  $T_e$  gas in the cluster rest frame ( $E' = (1+z)E$ ,  $\delta'_E = (1+z)\delta_E$ ), and the integral is again along the line of sight. Note,  $\Lambda(E', T_e)$  decreases steeply with  $z$  over the energy range of interest (usually in the range 0.5 to 10 keV), so that the detectability of a cluster for a given X-ray detector typically falls steeper than  $1/(1+z)^4$  in sharp contrast to the essentially redshift independence of the SZE signal.

Due to the different electron density dependencies of the observed SZE ( $\propto n_e$ ) and X-ray ( $\propto n_e^2$ ) emission, one can use the measurements to constrain the electron distribution, or at least constrain the parameters within a given model for the gas. One also needs the electron temperature which can be measured using X-ray spectroscopy. The determined gas distribution can then be compared with the measured angular distribution to solve for the distance to the cluster. A comparison with the mean redshift of the member galaxies gives the Hubble constant  $H_o$ .

The beauty of this technique for measuring the Hubble constant is that it is completely independent of other techniques, and that it can be used to measure distances at high redshifts. While the method depends only on well understood properties of fully ionized plasmas, there are several sources of uncertainty in the derivation of the Hubble constant for any particular cluster (e.g., see Birkinshaw 1999). The largest uncertainty is that we are making the assumption that the cluster size along the line of sight is comparable to its size in the plane of the sky. For this reason it is desirable to use a large survey of clusters to determine  $H_o$ . A large survey of perhaps a few hundred clusters with redshifts ranging from close by to beyond one would allow the technique to be used to trace the expansion history of the universe, providing a valuable independent check of the type Ia supernova results (e.g., Riess *et al.* 1998; Perlmutter *et al.* 1999).

## 2.2 Peculiar velocities

The line of sight velocity of a cluster with respect to the CMB rest frame, the peculiar velocity of the cluster, can be measured by separating the kinetic from the thermal SZE. From inspection of Fig. 1, it is clear that this is best done by observation at frequencies near the null of the thermal effect at  $\sim 218$  GHz. Such measurements offer the ability to measure the peculiar velocity of clusters at high redshifts which could be used to constrain the large scale gravitational perturbations to the Hubble flow. The intrinsic weakness of the effect make the observation of the effect challenging. Upper limits have been placed on the peculiar velocities of clusters (Holzapfel *et al.* 1997a), but a clear detection of the kinetic effect has not yet been obtained. The kinetic SZE is a unique and potentially powerful cosmological tool as it provides the only known way to measure large scale velocity fields at high redshift. We are likely to see continued progress in these difficult observations. Our SZE observations discussed later in this paper were made at 30 GHz where the kinetic effect is clearly of second order to the thermal effect, and it is therefore not discussed further here.

## 2.3 Baryon mass fraction of clusters; $\Omega_M$

A measurement of the SZE toward a cluster provides a measure of the mass of the intracluster medium, which is typically several times the mass responsible for the light from the galaxies. Combining the gas mass with a measure of the total mass determined either from gravitational lensing observations or from the virial theorem and the X-ray determined electron temperature, one can determine the fraction of the mass of the galaxy cluster contained in baryons. An estimate of the baryonic to total mass on the scale of massive galaxy clusters is important as it should represent the universal value; it is not believed that mass segregation occurs on the scales from which massive clusters condense  $\sim 1000$  Mpc<sup>3</sup>, although as noted below a small fraction of baryons ( $\sim 15\%$ ) are likely lost during the cluster formation process.

The universal mass fraction of baryons to total matter,  $\Omega_B/\Omega_M$  where  $\Omega \equiv \rho/\rho_c$ , and  $\rho_c$  is the critical density of the universe, can in turn be used to estimate  $\Omega_M$  given the value determined for  $\Omega_B$  from big bang nucleosynthesis calculations and the observed values for the primordial abundance of the light elements (Burles and Tytler 1998).

## 2.4 Cluster evolution; probing the high redshift universe

Perhaps the most powerful use of the SZE for cosmology will be to probe the high redshift universe. Sensitive, non-targeted surveys of large regions of the sky for the SZE will provide an inventory of clusters independent of redshift. The cut-off of the SZE cluster sample would be a lower mass cut-off set by the sensitivity of the observations; there would be no redshift cut-off. The sensitivity of a such a survey to cosmological parameters is shown in Fig. 2, where the predicted distribution in redshift of all clusters with masses greater than  $2 \times 10^{14} M_\odot$  is shown (Holder, Carlstrom, and Mohr 1999). A sufficiently sensitive SZE survey would also be able to image the ionized gas expected in filamentary large scale structure, particularly the filaments associated with the formation of clusters.

The use of the number density of clusters, particularly massive clusters, as a function of redshift has been used by a number of authors to estimate  $\Omega_M$  from X-ray surveys (e.g., Bahcall 1999). The possible use of SZE surveys to constrain  $\Omega_M$  has been investigated as well (Barbosa *et al.* 1996; Colafrancesco *et al.* 1997)

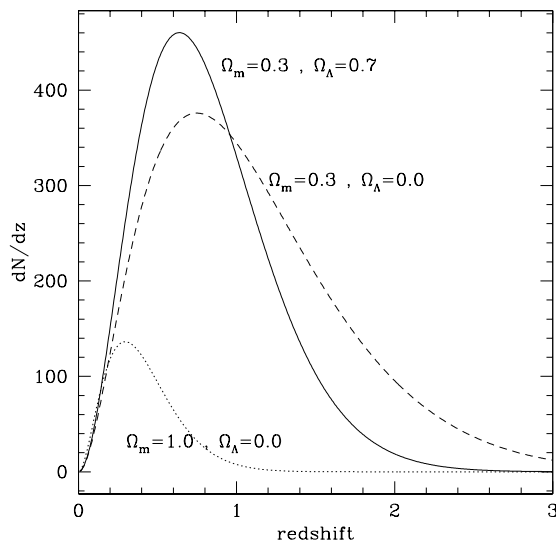


Figure 2: The predicted  $z$  distribution of clusters with masses greater  $2 \times 10^{14} M_{\odot}$  for several cosmologies (Holder and Carlstrom 1999). The numbers are for a 12 square degree patch of sky. Note the cosmological sensitivity of the cluster redshift distribution.

along with more recent studies which include the effect of the cluster gas evolution (Holder and Carlstrom 1999).

### 3 SZE Observations

#### 3.1 Previous observations

In the twenty years following the first papers by Sunyaev and Zel'dovich, there were few firm detections of the SZE despite a considerable amount of effort (Birkinshaw 1991). Over the last several years, however, observations of the effect have progressed from low S/N detections and upper limits to high confidence detections and detailed images. The dramatic increase in the quality of the observations is due to improvements both in low-noise detection systems and in observing techniques, usually using specialized instrumentation with which the systematics that often prevent one from obtaining the required sensitivity are carefully controlled. Such systematics include, for example, the spatial and temporal variations in the emission from the atmosphere and the surrounding ground.

A recent review of the observations can be found in Birkinshaw 1999. Here we briefly review a few of the results to provide the reader with a measure of the quality of the data presently available. We then concentrate on our own technique and imaging results.

The first measurements of the SZE were made with single dish radio telescopes. Successful detections were obtained, although the reported results show considerable scatter, reflecting the difficulty of the measurement. Recent state-of-the-art single dish observations at radio wavelengths (Herbig *et al.* 1995; Myers *et al.* 1997), millimeter wavelengths (Wilbanks *et al.* 1994; Holzapfel *et al.* 1997b) and submillimeter wavelengths (Lamarre *et al.* 1998) have resulted in significant detections of the effect and limited mapping.

Interferometric techniques have been used to produce high quality images of the SZE (e.g., Jones *et al.* 1993; Grainge *et al.* 1993; Carlstrom, Joy, and Grego 1996; Grainge *et al.* 1996; Carlstrom *et al.* 1998). As discussed in the next section, the high stability and spatial filtering made possible with interferometry is being exploited to make these observations.

### 3.2 Interferometry basics

The stability of interferometry is attractive for avoiding many of the systematics which can prevent one from imaging very weak emission. The ‘beam’ of a two-element interferometer – all arrays can be thought of as a collection of  $n(n - 1)/2$  two-element interferometers – is essentially a cosine corrugation on the sky; it is exactly analogous to a two slit interference pattern. The interferometer does the job of multiplying the sky brightness at the observing frequency by a cosine, integrating the product and producing the time average amplitude. The correlator performs the multiplication and time averaging. In practice two correlators are used to obtain the cosine and sine patterns. Simply put, the interferometer measures directly the Fourier transform of the sky at a spatial frequency given by  $B/\lambda$ , where  $B$  is the component of the vector connecting the two telescopes (the baseline) oriented perpendicular to the source. Of course, a range of baselines are actually being used at any one time due to the finite size of the apertures of the individual array elements; this simply reflects that the sky has been multiplied by the gain pattern (beam) of the individual telescopes or, equivalently, that the Fourier transform measured is the transform of the true sky brightness convolved with the transform of the beam of an array element.

That the Fourier transform measured is the transform of the sky brightness convolved with the transform of the beam of an individual element has important consequences. The transformed beam is the auto-convolution of the aperture, and thus it is identically zero beyond the diameter of the telescopes expressed in wavelengths. The interferometer is therefore only sensitive to angular scales (spatial frequencies) near  $B/\lambda$ . It is not sensitive to gradients in the atmospheric emission or other large scale emission features. There are several other features which allow an interferometer to achieve extremely low systematics. For example, only signals which correlate between array elements will lead to detected signal. For most interferometers, this means that the bulk of the sky noise for each element will not lead to signal. Amplifier gain instabilities for an interferometer will not lead to large offsets or false detections, although if severe they may lead to somewhat noisy signal amplitude. To remove the effects of offsets or drifts in the electronics as well as the correlation of spurious (non-celestial) sources of noise, the phase of the signal received at each telescope is modulated before the correlator and then the proper demodulation is applied to the output of the correlator.

Lastly, the spatial filtering of an interferometer allows the emission from radio point sources to be separated from the SZE emission. This is possible because at high angular resolution ( $< 10''$ ) the SZE contributes very little flux. This allows one to use long baselines – which give high angular resolution – to detect and monitor the flux of radio point sources while using short baselines to measure the SZE. Nearly simultaneous monitoring of the point sources is important as they are often time variable. The signal from the point sources is then easily removed, if they are not too strong, from the short baseline data which are sensitive to the SZE. Nevertheless, one would still prefer to operate at shorter radio wavelengths since the point sources typically have falling spectra ( $\sim \lambda^{0.7}$ ), while the SZE signal scales as ( $\lambda^{-2}$ ).

For the reasons given above, interferometers offer an ideal way to achieve high brightness sensitivity for extended low-surface brightness sources, at least at radio wavelengths. Most interferometers, however, were not designed for imaging low-surface brightness sources. Interferometers are traditionally built to obtain high angular resolution with large individual elements for maximum sensitivity to small scale emission. Galaxy clusters, on the other hand are large objects. Most of the SZE signal will be distributed smoothly on angular scales of an arcminute or more for even the most distant clusters, scales for which most existing interferometric arrays are simply not sensitive.

### 3.3 OVRO and BIMA interferometric imaging of the SZE

Our solution to matching the angular scales important for observations of distant galaxy clusters (a few arcminutes) with those provided by an interferometer is to use existing mm-wave arrays, which were also designed for high resolution, but to degrade the angular resolution by outfitting the arrays with cm-wave receivers. This solution has a number of attractive features in addition to matching the arcminute scales appropriate for SZE measurements of distant clusters. Specifically, we are able to use very low noise cm-wave receivers. We are able to secure large amounts of observing time during the summer months when the atmosphere is not ideal for mm-wave observations, but reasonable for cm-wave. As one might imagine, there are also a number of advantages to using telescopes which have surface and pointing accuracies ten times higher than needed.

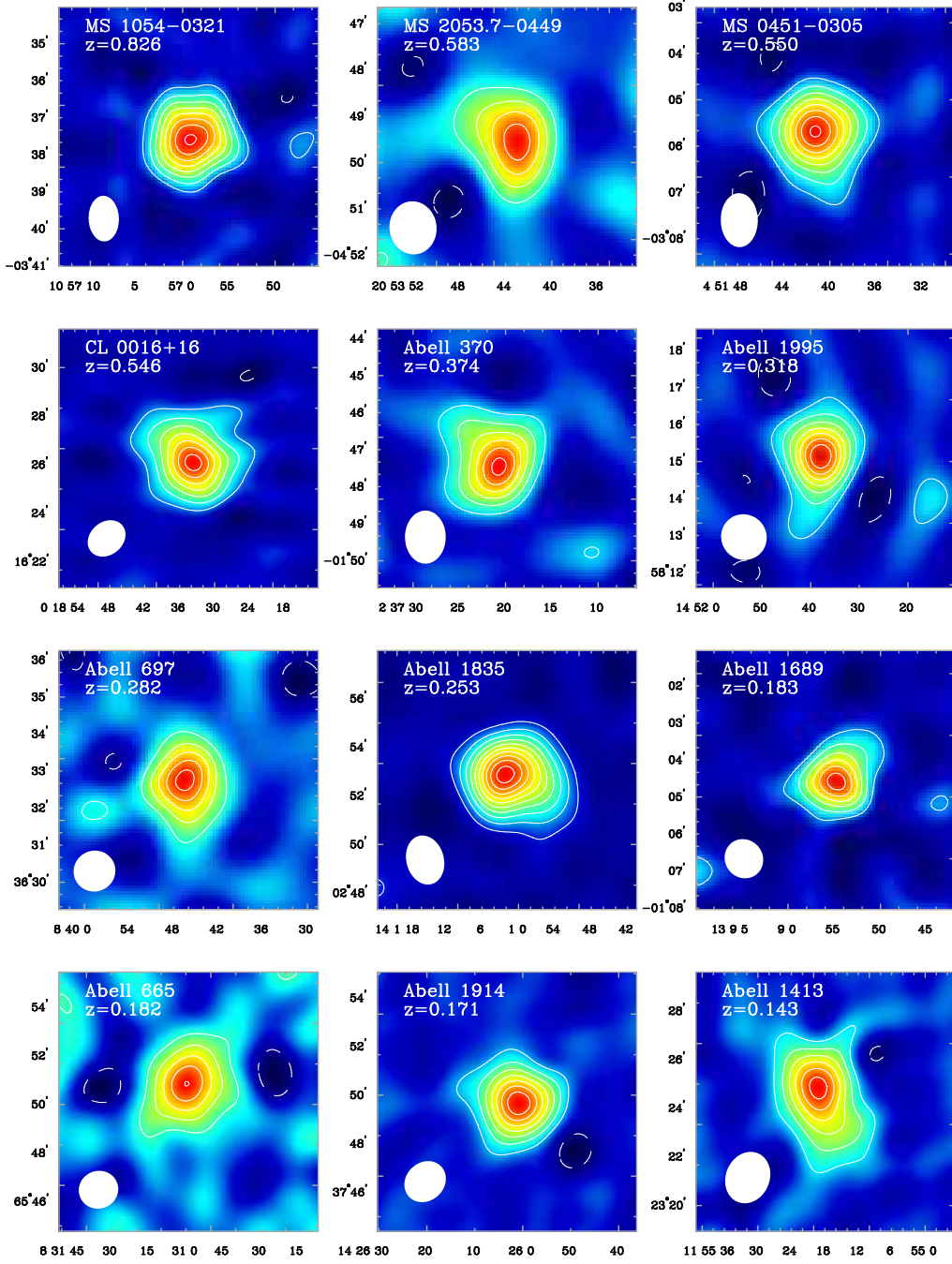


Figure 3: Images of the Sunyaev-Zel'dovich effect toward twelve distant clusters with redshifts spanning 0.83 (top left) to 0.14 (bottom right). The evenly spaced contours are multiples starting at  $\pm 1$  of  $1.5\sigma$  to  $3\sigma$  depending on the cluster, where  $\sigma$  is the rms noise level in the images. The noise levels range from 15 to  $40 \mu\text{K}$ . The data were taken with the OVRO and BIMA mm-arrays outfitted with low-noise cm-wave receivers. The filled ellipse shown in the bottom left corner of each panel represents the FWHM of the effective resolution used to make these images.

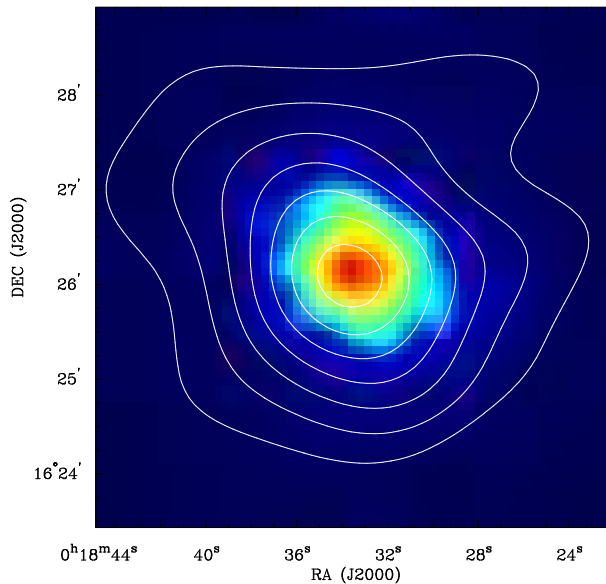


Figure 4: The Sunyaev-Zel'dovich effect (contours) overlaid on the X-ray emission (false color) for the galaxy cluster CL 0016+16. The SZE data were obtained with the OVRO and BIMA mm-arrays. The X-ray data were obtained with the ROSAT PSPC.

Over the last few summers we have thus installed low-noise, HEMT amplifier based receivers on the OVRO<sup>1</sup> and BIMA<sup>2</sup> mm-wave arrays in California. The receivers operate from 26 - 36 GHz (30 GHz corresponds to 1 cm), and down convert the signal to the standard intermediate frequencies used at the two arrays. All of the normal array correlators, electronics, and software are used. About 1 GHz can be processed at one time with the standard observatory electronics. Data are taken from array configurations in which roughly half the baselines are sensitive only to point sources and the other half are as short as possible for maximum sensitivity to the SZE.

In Fig. 3 we show a subset of the 27 clusters that we imaged so far using the OVRO and BIMA arrays. Contaminating emission from radio point sources was removed before making these images. The short baseline data were emphasized when these images were made to enhance the surface brightness sensitivity. The data do contain significant information at higher resolution. A catalog of the point sources we measured toward our SZE imaged clusters can be found in Cooray *et al.* 1998. Fig. 3 illustrates the high quality data we have been able to obtain. The typical integration time used for each cluster is about 45 hours, which when one includes calibration and other overheads takes roughly 8 to 10 transits of the source.

Fig. 3 also clearly demonstrates the independence of the SZE on redshift. All of the clusters shown have similar high X-ray luminosities and, as can be seen, the strength of the SZE is similar for each one. For the associated X-ray emission, however, the rate of received photons falls off drastically with redshift.

The SZE image is shown (contours) on the corresponding X-ray emission in Fig. 4. As expected, the SZE which traces the density of the cluster gas is less centrally peaked than the X-ray emission which traces the square of the density.

<sup>1</sup>An array of six 10.4 m mm-wave telescopes located in the Owens Valley, CA and operated by Caltech.

<sup>2</sup>An array of ten 6.1 m mm-wave telescopes located at Hat Creek, California and operated by the Berkeley-Illinois-Maryland-Association



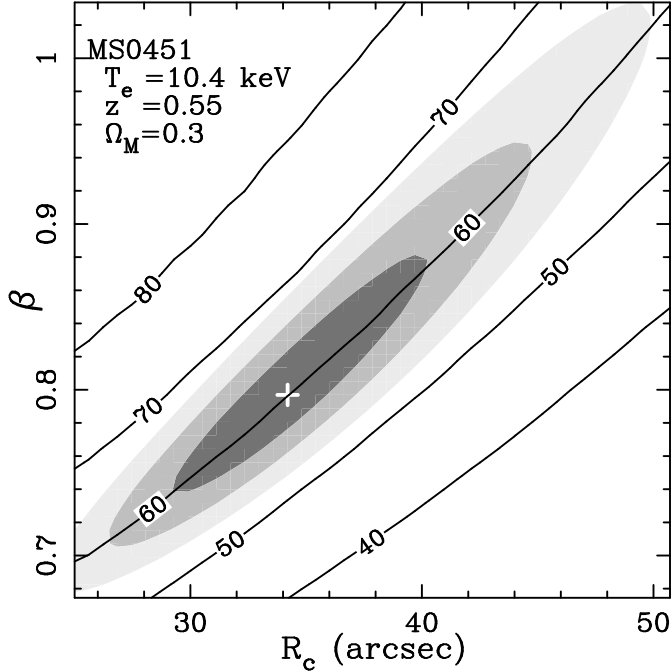


Figure 5: The derived Hubble constant in units of  $km\ s^{-1}Mpc^{-1}$  is shown as contours from joint fits to Sunyaev-Zel'dovich data and X-ray data to the cluster MS 0451-0305. The 1,2 and  $3\sigma$  confidence regions for the fit parameters  $\beta$  and  $R_c$  are shown in greyscale. Note that the value of the fitted Hubble constant is essentially insensitive to the clear degeneracy between the fitted values of  $\beta$  and  $R_c$ .

## 4 Results

We have been developing methods for best extracting the cosmological parameters from our SZE data. One has to keep in mind that the images shown in Fig. 3, while they give a direct indication of the data quality, have been heavily filtered by the response of the interferometer. Therefore, we do all of our analyses in the Fourier domain where the data are actually measured.

We fit models for the cluster gas distribution to our data by first constructing a realization of the model, projecting it in the plane of the sky, multiplying it by the angular gain response of our instrument (the beam of an array element), and then Fourier transforming it to the spatial frequency of our data points. A comparison of the model Fourier transform points and the data points is used to construct the likelihood of the model.

For a suitable model we start with a standard  $\beta$ -model for the gas distribution

$$n_e(r) = n_e(0) \left( 1 + \frac{r^2}{R_c^2} \right)^{-3\beta/2} \quad (3)$$

where  $n_e(0)$  is the central electron density,  $R_c$  is the core radius, and  $\beta$  a power law index. In practice, we generalize this to be elliptical, fitting for the position angle and major/minor axes ratio. We also fit the location of the cluster as well as the locations and fluxes of any radio point sources. We assume the gas is isothermal. For each set of parameters a likelihood (actually a  $\chi^2$  since the noise is Gaussian) is obtained.

When X-ray data is also used in the analyses, a similar procedure is followed and the joint likelihood is obtained.

### 4.1 Hubble constant

We are performing joint analyses of X-ray and our SZE data to determine the distance to each cluster. The result of such a derivation for the cluster MS 0451-0305 is shown in Fig. 5 (Reese *et al.* 1999). The values

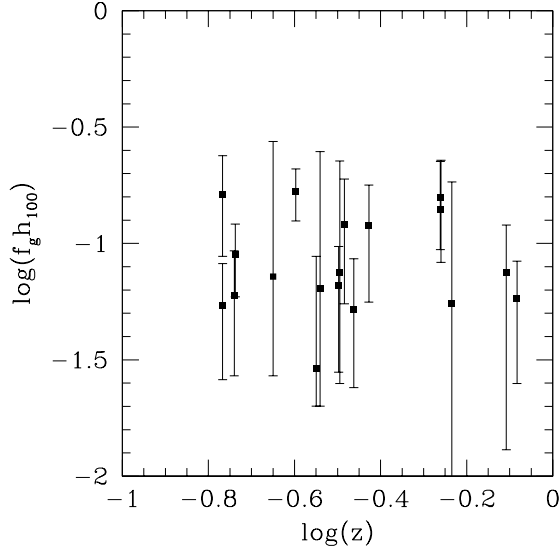


Figure 6: The gas mass fraction for galaxy clusters derived from OVRO and BIMA Sunyaev-Zel’dovich effect data as a function of redshift.

for  $H_o$  (in units of  $km\ s^{-1}Mpc^{-1}$ ) are shown as contours on a plot of the model parameters  $\beta$  and  $R_c$ . The 1, 2 and 3 $\sigma$  confidence intervals are shown by the greyscale regions. Note the striking independence of the derived value of  $H_o$  along the clear degeneracy in the fits to these model parameters.

There are uncertainties in the absolute calibration of both the SZE and X-ray data. However, the largest uncertainty in the derived  $H_o$  for any one cluster is the unknown cluster aspect ratio, since we implicitly assume the cluster dimension along the line of sight is equal to its dimension across the line of sight. That our analyses of MS 0451-0305 gives a value for  $H_o$  that is so close to the currently accepted range for  $H_o$  is somewhat fortuitous. To obtain a trustworthy estimate for  $H_o$  using the SZE one must obtain a large sample of distances and be careful of selection effects. We are in the process of conducting such a survey now. In his recent review, Birkinshaw found the average for all published SZE derived values of  $H_o$  to be  $60 \pm 10\ km\ s^{-1}Mpc^{-1}$  (Birkinshaw 1999). Note, however, as Birkinshaw points out, that the underlying observations share common and fairly uncertain calibrations.

## 4.2 Cluster gas mass fractions and constraints on $\Omega_M$

We have determined the gas mass fractions for 18 clusters using only our SZE data and electron temperatures derived from X-ray spectroscopy (Grego 1999; Grego *et al.* 1999a). We did not use X-ray imaging data, and in that sense our results provide a test of similar analyses done on X-ray data sets. Details of our technique in which we account for the expected bias of the gas mass fraction in the core region of a cluster can also be found in Grego *et al.* 1999b. The resulting gas mass fractions as a function of redshift are shown in Fig. 6. In most of the clusters, the uncertainty is dominated by poorly constrained electron temperatures.

The degeneracy in the fit parameters  $R_c$  and  $\beta$  is worse than that shown in Fig. 5 since we are not using the X-ray data to help constrain the fits. We find that the derived gas mass and the gas mass fraction are insensitive to the particular values of  $R_c$  and  $\beta$  within the region of acceptable fits, as long as these quantities are only calculated within about an arcminute radius region. This is not surprising, as the SZE signal is directly proportional to the mass and our data constrains the signal well on these scales. We relate the gas fractions we derive at arcminute scales to the expected gas fractions near the cluster virial radius using scaling relations derived from numerical simulations of cluster formation (Evrard 1997).

The eighteen clusters range in redshift from 0.171 to 0.826. Assuming an open  $\Omega_M = 0.3$ ,  $\Omega_\Lambda = 0$  cosmology, we find  $f_g h_{100} = 0.075^{+0.007}_{-0.010}$  scaled to  $r_{500}$ , the radius at which the overdensity of the cluster is 500, nearly the virial radius. Using the six clusters with redshifts less than 0.26, so that the cosmology we

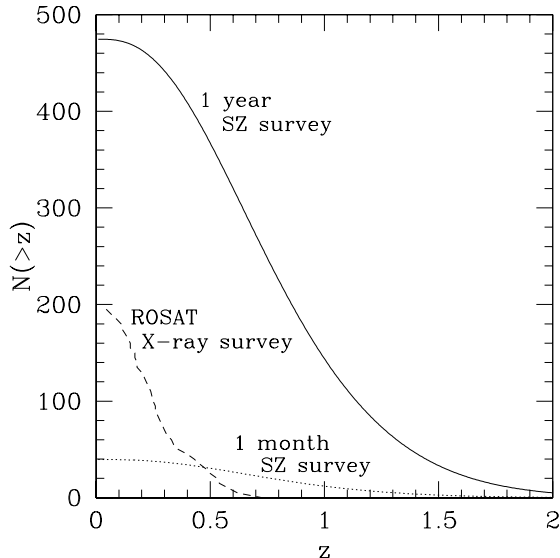


Figure 7: The expected number of clusters detected with an array of 10 2.5-m telescopes operating at 1 cm and with a correlation bandwidth of 8 GHz conducting a survey for one month– 1 deg<sup>2</sup>– (dotted) and for one year– 10 deg<sup>2</sup>– (solid). The predictions are based on a  $\Omega_\Lambda = 0.7$ ,  $\Omega_M = 0.3$  flat CDM cosmology; the predicted numbers are comparable for an open CDM model. The resulting sample of clusters would have more than 300 clusters with  $z > 0.5$  and more than 100 with  $z > 1$ . For comparison, we show the cluster sample from a deep, serendipitous, X-ray survey of  $\sim 160$  deg<sup>2</sup> carried out using archival ROSAT PSPC images.

assume will have little effect on the gas mass fractions derived, we find  $f_g h_{100} = 0.085^{+0.011}_{-0.015}$ , again scaled to  $r_{500}$ .

Our results are in good agreement with those derived by Myers *et al.* 1997 for a sample of 3 nearby clusters, and also with values derived from X-ray emission (David, Jones, and Forman 1995; Mohr, Mathiesen, and Evrard 1999), suggesting that systematic differences between the methods, like the clumping of intracluster gas, are not severe.

Assuming that the baryonic mass fraction for clusters reflects the universal value and using the constraint on  $\Omega_B$  determined from BBN and primordial abundance measurements (Burles and Tytler 1998),  $\Omega_B h_{100}^2 = 0.019 \pm 0.001$ , the low redshift gas mass fractions imply  $\Omega_M h_{100} \leq \Omega_B / f_g = 0.22^{+0.05}_{-0.03}$ . A best guess of  $\Omega_M$  can be made by attempting to account for the baryons lost during the cluster formation process (15%) and for the baryons contained in the galaxies, as well as using a best guess for the Hubble constant. This gives  $\Omega_M \sim 0.23^{+0.06}_{-0.04} h_{65}^{-1}$ . The uncertainties should be taken with caution as they do not reflect the uncertainties in the assumptions used to extrapolate from  $\Omega_B / f_g$  to  $\Omega_M$ .

## 5 Discussion and Future Plans

We are able to obtain high quality imaging data of the SZE toward distant galaxy clusters. Our constraint on the gas mass fractions of galaxy clusters provides further support that we live in a low  $\Omega_M$  universe. Our  $H_o$  results are still preliminary, but show promise of providing a good independent estimate for the expansion of the universe.

We are continuing to work on our analysis tools, including testing thoroughly the effects of our assumptions such as the isothermality of the cluster gas and the limits of  $\beta$ -models.

We are still a long way from being able to constrain whether the universe is accelerating or not. And, even though our sensitivity is quite high, we are not yet in a position to conduct large sensitive, non-targeted surveys for the SZE over large regions of the sky. We have, however, clearly demonstrated the feasibility of using similar interferometric techniques to conduct such a survey.

A dedicated array with 10 elements of 2.5 m diameter and using our cm-wave receivers would increase the speed of system dramatically. In Fig. 7 we show the expected number of clusters detected with such an instrument (see Holder, Carlstrom, and Mohr 1999). One month of observing with this array would deliver more clusters with redshifts higher than  $z \sim 0.5$  than are found in the deepest, large area X-ray cluster catalogs (Vikhlinin *et al.* 1998). The plot assumes a  $\Omega_m = 0.3$ ,  $\Omega_\Lambda = 0.7$  cosmological model; if  $\Omega_\Lambda = 0$  the counts are comparable (see Fig. 2).

The potential of using the SZE as a tool to help determine the cosmological parameters is now being realized nearly three decades after it was first proposed. We expect improvements to move forward at a rapid pace with sensitive SZE surveys of the the high redshift universe starting in the next few years.

We thank the OVRO and BIMA observatories for their crucial contributions to the SZE observations. JC thanks organizers of the symposium for a remarkably informative and enjoyable symposium. JC acknowledges support from a NSF-YI grant and the David and Lucile Packard Foundation.

## References

- Bahcall, N. 1999. Cosmology with Clusters of Galaxies. In Bergstrom, L., Carlson, P., and Fransson, C., editors, *Nobel Symposium on Particle Physics and the Universe*, Sweden. Physics Scripta – astro-ph/9901076.
- Barbosa, D., Bartlett, J., Blanchard, A., and Oukbir, J. 1996, A&A, **314**, 13.
- Birkinshaw, M. 1991, *Physical Cosmology*, ed. J. Tran Thanh Yan, Editions Frontiers, page 177.
- Birkinshaw, M. 1999, Physics Reports, **310**, 97.
- Burles, S. and Tytler, D. 1998, ApJ, **507**, 732.
- Carlstrom, J. E., Grego, L., Holzapfel, W. L., and Joy, M. 1998, Eighteenth Texas Symposium on Relativistic Astrophysics and Cosmology, ed A. Olinto, J. Frieman, and D. Schramm, World Scientific, page 261.
- Carlstrom, J. E., Joy, M., and Grego, L. E. 1996, ApJ, **456**, L75.
- Colafrancesco, S., Mazzotta, P., Rephaeli, Y., and Vittorio, N. 1997, ApJ, **479**, 1.
- Cooray, A. R., Grego, L., Holzapfel, W. L., Joy, M., and Carlstrom, J. E. 1998, AJ, **115**, 1388.
- David, L., Jones, C., and Forman, W. 1995, ApJ, **445**, 578.
- Evrard, A. 1997, MNRAS, **292**, 289.
- Grainge, K., Jones, M., Pooley, G., Saunders, R., Baker, J., Haynes, T., and Edge, A. 1996, MNRAS, **278**, L17.
- Grainge, K., Jones, M., Pooley, G., Saunders, R., and Edge, A. 1993, MNRAS, **265**, L57.
- Grego, L. 1999. *Galaxy Cluster Gas Fractions from Interferometric Measurements of the Sunyaev-Zel'dovich Effect*. PhD thesis, Caltech.
- Grego, L., Carlstrom, J. E., Joy, M. K., Reese, E. D., Holder, G. P., Patel, S., Cooray, A. R., and Holzapfel, W. L. 1999a, ApJ – submitted.
- Grego, L., Carlstrom, J. E., Joy, M. K., Reese, E. D., Holder, G. P., Patel, S., Cooray, A. R., and Holzapfel, W. L. 1999b, ApJ – submitted.
- Herbig, T., Lawrence, C. R., Readhead, A. C. S., and Gulkis, S. 1995, ApJ, **449**, L5.
- Holder, G. and Carlstrom, J. 1999. The Sunyaev-Zeldovich Effect as Microwave Foreground and Probe of Cosmology. In de Oliveira-Costa, A. and Tegmark, M., editors, *Microwave Foregrounds*, San Francisco. ASP– astro-ph/9904220.
- Holder, G., Carlstrom, J., and Mohr, J. 1999, ApJ – in preparation.
- Holzapfel, W. L., Ade, P. A. R., Church, S. E., Mouskops, P. D., Rephaeli, Y., Wilbanks, T. M., and Lange, A. E. 1997a, ApJ, **481**, 35.
- Holzapfel, W. L. *et al.* 1997b, ApJ, **480**, 449.
- Jones, M. *et al.* 1993, Nature, **365**, 320.
- Lamarre, J. M. *et al.* 1998, ApJ, **507**, L5.
- Mohr, J., Mathiesen, B., and Evrard, A. 1999, ApJ, **517**, – astro-ph/9901281.
- Myers, S. T., Baker, J. E., Readhead, S., A. C., Leitch, E. M., and Herbig, T. 1997, ApJ, **485**, 1.
- Perlmutter, S. *et al.* 1999, ApJ, pages accepted, see astro-ph/9812133.

Reese, E. D. *et al.* 1999, ApJ – in preparation.

Rephaeli, Y. 1995, ARAA, **33**, 541.

Riess, A. G. *et al.* 1998, AJ, **116**, 1009.

Sunyaev, R. and Zel'dovich, Y. 1970, Comments Astrophys. Space Phys., **2**, 66.

Sunyaev, R. and Zel'dovich, Y. 1972, Comments Astrophys. Space Phys., **4**, 173.

Sunyaev, R. and Zel'dovich, Y. 1980, ARAA, **18**, 537.

Vikhlinin, A., McNamara, B., Forman, W., Jones, C., Quintana, H., and Hornstrup, A. 1998, ApJ, **502**, 558.

Wilbanks, T. M., Ade, P. A. R., Fischer, M. L., Holzappel, W. L., and Lange, A. E. 1994, ApJ, **427**, L75.